Multi-hazard Risk Mapping with Machine Learning

20 October 2022

Colombo, Sri Lanka

Peniel Adounkpe, Surajit Ghosh, Giriraj Amarnath

CGIAR
INITIATIVE ON
Climate Resilience

Authors

Peniel Adounkpe[1], Surajit Ghosh[1], Giriraj Amarnath[1]

[1] International Water Management Institute (IWMI), Battaramulla, Sri Lanka

Suggested Citation

Adounkpe P, Ghosh S, Amarnath G. 2022. *Multi-hazard Risk Mapping with Machine Learning*. CGIAR Climate Resilience Initiative.

Acknowledgments

This work was carried out with support from the CGIAR Initiative on Climate Resilience, ClimBeR. We would like to thank all funders who supported this research through their contributions to the CGIAR Trust Fund.

Table of Contents

1. Introduction

The African continent is prone to a wide variety of natural hazards. Hydrometeorological hazards (such as floods, droughts, heat waves, storms, and others.) account for most of the natural disasters in the region (van Niekerk et al., 2022). Droughts are a perennial problem and affect millions of people across the Horn of Africa, Sahel and southern Africa. Floods disrupt the lives and livelihoods of populations across many economic centers and countries and severely affect poor people (World Bank Group, 2016). In the 6th IPCC report, experts reaffirm that climate change is expected to dramatically increase the intensity and occurrence of extreme events around the globe. These events are expected to severely impact the most vulnerable populations (IPCC, 2022).

Since the food crisis of 2008 and the increased frequency of extreme weather events, such as floods and droughts, there has been renewed interest in finding alternative solutions to guarantee to improve the resilience of Ghana's inhabitants (Braun 2008; UN 2011). Flood disasters have killed 415 people, affected 3,885,695 people and caused around 108,000,000 USD of damage; drought disasters have affected 12,512,000 people and have caused 100,000 USD of damage (EM-DAT, 2008). Therefore, earlier identification of natural hazard risk areas becomes crucial for planning humanitarian responses and executing risk reduction programs and policies efficiently.

The term "risk" is used in this study according to the IPCC definition. Risk provides an understanding the increasingly severe, interconnected and often irreversible impacts of climate change on ecosystems, biodiversity, and human systems; differing impacts across regions, sectors and communities. In the context of climate change, risk can arise from the dynamic interactions among climate-related hazards (hazard susceptibility) and the exposure and vulnerability of affected human and ecological systems (IPCC, 2022).

Studies in Ghana highlight that the most vulnerable regions to climate change are the northern, Upper East and Upper West regions. Al-Hassan surveyed 320 farm households, complemented with secondary data on rainfall and temperature and used the livelihood vulnerability index, to highlight access and utilization of water resources (Al-Hassan, 2013). He found that the Northern Region is the most exposed region to climate change and variability. Upper West Region is the most sensitive to climate change and variability, especially regarding water stress; the Upper East Region has the least adaptive capacity. Antwi-Agyei's study identified differences across and within ten regions of Ghana and the proposed methodological steps to improve drought sensitivity and vulnerability assessments in dynamic dryland farming systems (Antwi-Agyei, 2011). The vulnerability of crop production to drought in Ghana has discernible geographical and socioeconomic patterns, with the Northern, Upper West and Upper East

regions being the most vulnerable. These regions have the lowest adaptive capacity due to low socioeconomic development and economies based on rain-fed agriculture.

Rehman reveals the gap between methods and approaches for evaluating vulnerability to hazards using high-resolution data and a multidimensional approach for assessing vulnerability (Rehman, 2019). Several recent studies highlight the importance of ML models for natural hazard susceptibility mapping (Pourghasemi et al., 2020; Rahmati et al., 2019; Yousefi et al., 2020; Islam, 2021; Rahmati, 2020; Saha, 2021). RF and SVM models stand out when classifying natural hazards (specifically floods and droughts) with earth observation data (EO). Many EO datasets were used and processed as the ML model's input data. The most frequent ones were elevation (and its derivates such as topographic wetness index, aspect and slope), temperature, rainfall, distance from faults, geology type, land use type, distance from the river, and distance from nearest road and soil type. These studies also started by collecting a database of past hazards of each studied region. The following step was to split that database using 70% of the hazard event to train the ML model and 30% for their validation using Areas-Under-the-Curves (AUC). Finally, the best model was selected to map the hazard's susceptibility. The idea behind this research is to compare the models to each other, and their performances to a basic ML algorithm such as Logistic Regression (LR) used as the benchmark model. This work does not only integrate the susceptibility of the hazard but also takes into account the populations' exposure and vulnerability to effectively determine the risk of the hazard. Furthermore, this study determines the population's vulnerability according to its sensitivity and adaptation capacity.

This study aims to use ML models (LR, RF and SVM) to map flood and drought susceptibility and add exposure and vulnerability data to obtain flood and drought risk maps in Ghana. To do this, (1) the best ML model for flood and drought classification was determined and used to map flood and drought susceptibility, (2) a vulnerability analysis was conducted with socioeconomic surveys, and (3) an exposure analysis was derived using population density data, and (4) a multi-hazard risk map was the product of the susceptibility, the vulnerability and the exposure.

2. Methods and data

Study area

Ghana is a country in West Africa located between latitudes 4.5°N and 11.5°N and longitudes 3.5°W and 1.5°E. More recent literature shows a new organization of Ghana's regions, counting them up to 16: Ahafo, Ashanti, Bono, Bono East, Central, Eastern, Greater Accra, Northern, North East, Oti, Savannah, Upper

East, Upper West, Volta and Western (GSS, 2022). But in this study, the 10 classical regions were used, as shown in **Figure 1**. Ghana's major cities are Accra, Kumasi, Tamale, Tema, Koforidua and Cape Coast. From the same survey, Ghana's total population was mentioned as about 30 million. Ghana has 4 main agro-ecological zones: coastal, forest, transition and savannah (Amekudzi et al., 2015). Ghana's climate is tropical and strongly influenced by the West Africa monsoon winds. Its average temperatures range from 22°C to 32°C, and its annual rainfalls range from 700mm to 2030mm (Kabo-Bah et al., 2016).

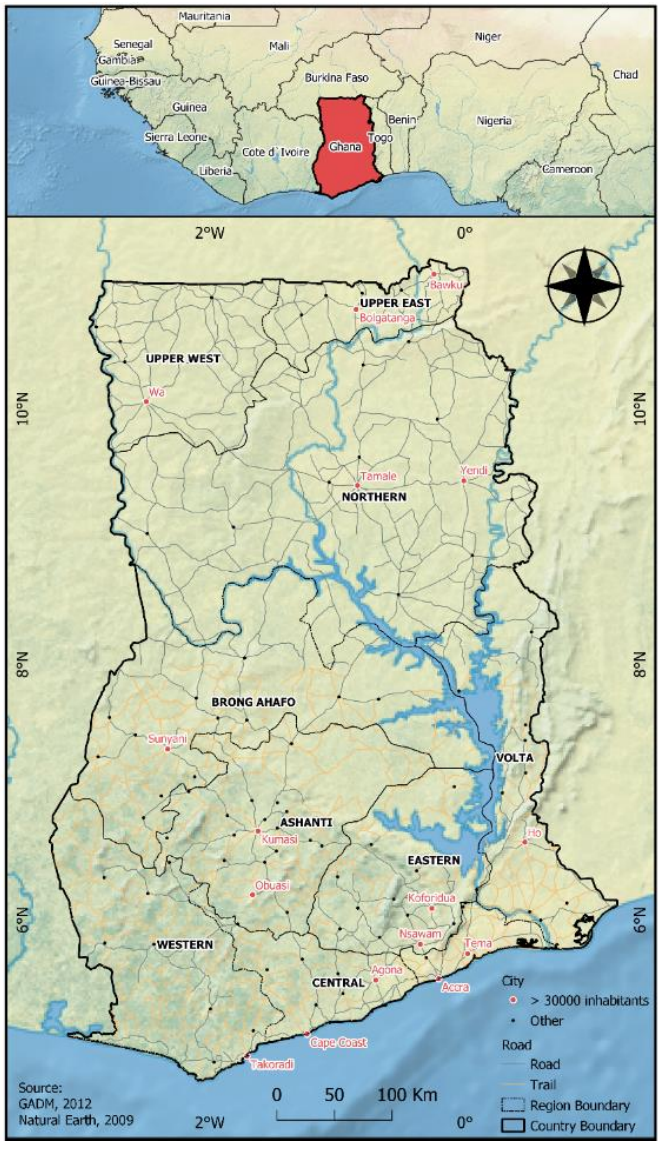

Figure 1: *Map of Ghana's boundaries, major cities and roads*

Data and Tools

A large number of datasets were required to complete this study. The table below presents the datasets used in this study. This study was done using Python modules in Google Colab's (Bisong, 2019) programming interface.

Table 1: *Group of indicators, category and source of datasets*

Risk factor	Indicator	Data		Organization (Citation)
Susceptibility	Natural Hazards	Flood locations	EM-DAT International Disaster Database from 1989 to 2022	CRED (EM-DAT, 2008)
			ECMWF FloodList from 2013 to 2022	ECMWF (FloodList, 2022)
		Drought locations	0.05° resolution CHIRPS monthly precipitation from 1981 to 2021	USGS & CHC (Funk, C. et al., 2015)
	Topography	30m resolution digital elevation model		CIAT-CSI SRTM (Jarvis et al., 2008)
	Meteorological	0.05° resolution CHIRPS monthly precipitation from 1981 to 2021		USGS & CHC (Funk et al., 2015)
		0.4° resolution monthly temperature from 1981 to 2020		ECMWF (Dee et al., 2011)
	Hydrological	River & water body		DCW, 2006 (Langaas, 1995)
	Surface Attributes	2km resolution Land cover		USGS (Tappan et al., 2016)
		0.5° resolution Soil cover		ISRIC (Niels, 2010)
Exposure	Demography	1km resolution spatial distribution of population density in 2020, Ghana		(WorldPop, 2018)
Vulnerability	Administrative Boundaries	Ghana boundary and regions		(GADM, 2012)
	Sensitivity and Adaptive Capacity	Ghana Living Standard Survey (GLSS 7)		(GSS, 2019)
		Road		DCW, 2006 (Langaas, 1995)

Methodology

The research workflow summarizes the different analysis performed in this study. The main steps were the natural hazard identification (finding flood and drought occurrences in Ghana), the raster preprocessing (preprocessing geospatial data into rasters with same characteristics), the natural hazard susceptibility mapping (training and validating ML models; selecting the best performing model and mapping flood and drought susceptibility), vulnerability analysis (analyzing the socio-economic situation

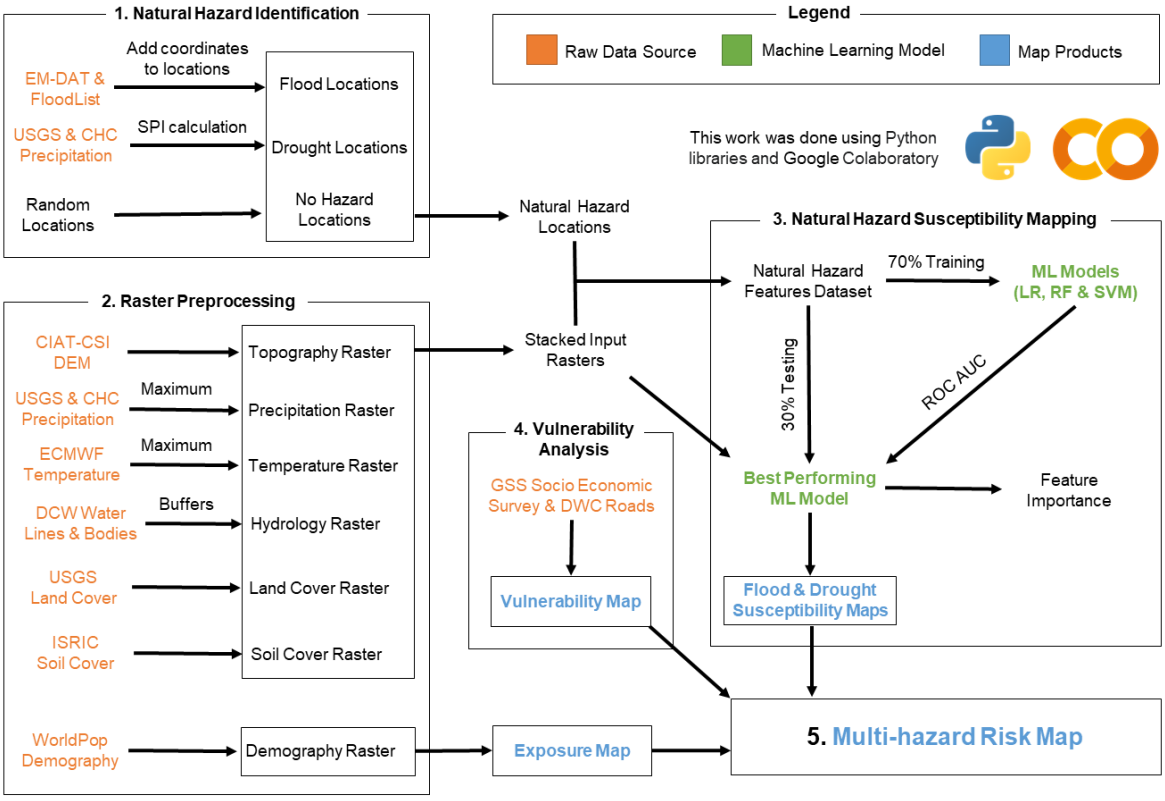

of Ghana regions) and the multi-hazard risk mapping.

***Figure 2**: Research Workflow for mapping multi-hazard risk with machine learning*

Natural Hazard Identification

After downloading all the required datasets for this research from different sources, as shown in **Table 1**, the goal was to find where natural hazards (flood and drought) occurred in Ghana. The flood locations were obtained from two different datasets: EM-DAT and FloodList. Geospatial references were added to the EM-DAT database containing names of flooded districts in Ghana. A search was done on the FloodList website to filter flood reports in Ghana, and spatial references were added to the districts mentioned in

the reports. The drought locations were obtained by calculating Ghana's 12-month Standardized Precipitation Index (SPI) using a precipitation dataset. The lowest values of SPI between 1981 and 2021 were selected, all values were extracted, and nearby drought locations were clustered.

Raster Preprocessing

Downloaded datasets were preprocessed into GeoTIFF format with the same extent, same resolution, same coordinate names and no missing values. The topography dataset was obtained by merging multiple SRTM rasters covering Ghana's boundary. The maximum monthly precipitations and temperatures over Ghana were computed. Precipitation, temperature, land cover, soil cover and demography datasets were converted to have the same attributes as the topography dataset because of its higher resolution. The hydrology (distance from the river) raster was obtained by applying distance buffers (2 to 10 km) to rivers in Ghana. The training/testing dataset was obtained after stacking the preprocessed rasters (except demography) and extracting the indicator values of each natural hazard location.

Natural Hazard Susceptibility Mapping

The three ML models used for this research were Random Forest (RF), Support Vector Machine (SVM) and Logistic Regression (LR). The input variables of the ML models were the topography, precipitation, temperature, hydrology (distance from the river), land cover and soil cover features of the training/testing dataset. The target variable was its hazard type feature. The training/testing dataset was partitioned into a 0.7/0.3 ratio and fed into the ML models for classifying hazard locations (flood and drought) and no hazard locations. The best-performing models for each natural hazard were selected to map the flood and drought susceptibility maps after evaluating AUC (Area Under the Curve) and ROC (Receiver Operating Characteristics). ROC is a probability curve, and AUC represents the degree or measure of separability. This evaluation metric benefits multi-class classification problems (Hajian-Tilaki, 2013). The higher the AUC, the higher the model's performance. The contribution of each indicator for the best model was also extracted.

Vulnerability Analysis

The vulnerability was obtained in the majority from the Ghana Living Standards Survey (GLSS 7). The vulnerability indicators were grouped into two main categories: sensitivity (socio-economy and livelihood) and adaptive capacity (human resources, economic security, infrastructure and basic facilities). The selected variables were heavily inspired by Bera's study on vulnerability and risk assessment to climate

change (Bera et al., 2022). The table below resumes the vulnerability variables used associated with each indicator.

***Table 2**: Vulnerability variables and indicators*

Indicators	**Indicators**	**Variables**
Sensitivity	Socio-economy	Food security (percentage of total food expenditure)
		Poverty (percentage of persons under the poverty line)
	Livelihood	Dependency on agriculture (percentage of labours relative to total population)
		Percentage of marginal workers
Adaptive Capacity	Human resource	Literacy rate
	Economic security	Percentage of salaried workers
		Household ownership (percentage of households owning a home)
		Household assets (percentage of total expenditure on clothing and furnishing)
	Infrastructure	Percentage of pukka house materials (outer wall, floor and roof)
		Road density (road density percentage) *
	Basic facilities	Sanitation (percentage of households with toilet)
		Electricity (percentage of households with connections)
		Safe drinking water (percentage of households with safe drinking water)

** from DCW road dataset*

The vulnerability was obtained using the formula below (Füssel and Klein, 2006):

$$Vulnerability = Sensitivity * (1 - Adaptive\ Capacity)$$

Hazard Risk Mapping

The exposure map was obtained using world population data. This demographic data originates from the 2020 estimates of numbers of people per grid square, with national totals adjusted to match UN population division estimates. The exposure map was obtained after setting the maximum population density to 40 persons per square km to integrate the lower density populations. The exposure raster values were then normalized between 0 and 1.

The risk of each natural hazard was obtained by multiplying the hazard susceptibility, the hazard exposure and the population vulnerability to natural hazards:

$$Risk\ (R)\ =\ Susceptibility\ (S)\ *\ Exposure\ (E)\ *\ Vulnerability\ (V)$$

The flood and drought risks were classified into 4 categories (low risk, flood, drought and both) depending on their risk values to obtain the multi-hazard risk map.

3. Results and discussion

Results

Natural Hazard Identification

A total of 150 flood locations were identified, with 108 from the EM-DAT database and 44 from the FloodList website. After SPI calculation and location clustering, 244 drought locations were identified. Precisely 204 locations with no flood and drought hazards were randomly selected. Overall, 598 locations were used to train and validate the ML models. Most of the drought locations can be found in the Central, Western and Upper West regions of Ghana. The Greater Accra region has the most flood events, followed by the cities of Kumasi, Tamale, Bolgatanga and Bawku.

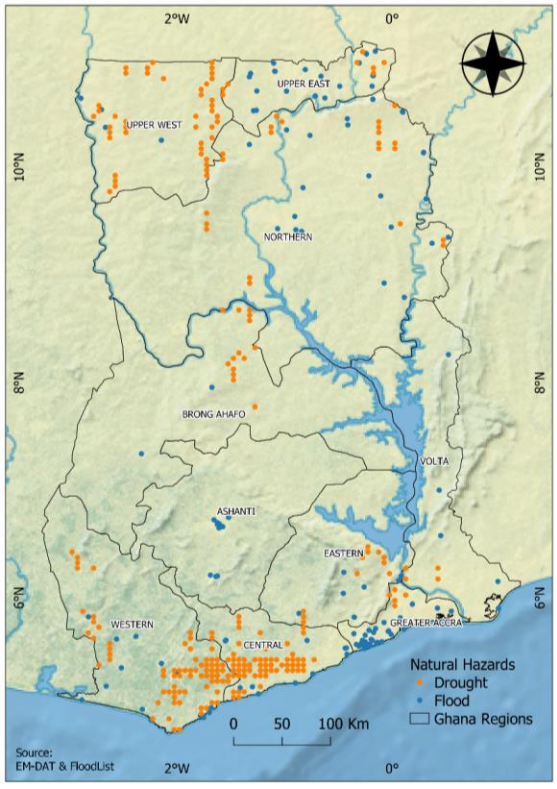

Figure 3: *Flood and drought locations in Ghana*

Raster Preprocessing

The 7 rasters (topographic, precipitation, temperature, hydrology/distance to river, land cover, soil cover and demography) of 7800x5400 pixels cover Ghana's extent. Ghana's topography is composed primarily of low plains, with a significant variation of the elevation in the south-central areas. The highest maximum precipitations are recorded in the South, while the highest maximum temperatures are in the north. The Northern areas are mainly covered with savannas and various plantations, and the Southern areas are mostly forested and sandy. The Southern areas of Ghana are the most densely populated.

Natural Hazard Susceptibility Mapping

The sampled dataset contains 598 rows representing all hazard locations and 7 columns consisting of topography, precipitation, temperature, hydrology, land cover, soil cover and hazard type. The ML models were validated using AUC and ROC. RF was the best model for predicting flood and drought events. The respective AUC of the RF, SVM and LR for flood prediction were 0.84, 0.82 and 0.82. The RF and SVM models of the flood events performed slightly better than those of the drought events. The LR model had a pronounced decline in performance when classifying drought events. The respective AUC of the RF, SVM and LR for drought prediction were 0.82, 0.81 and 0.70.

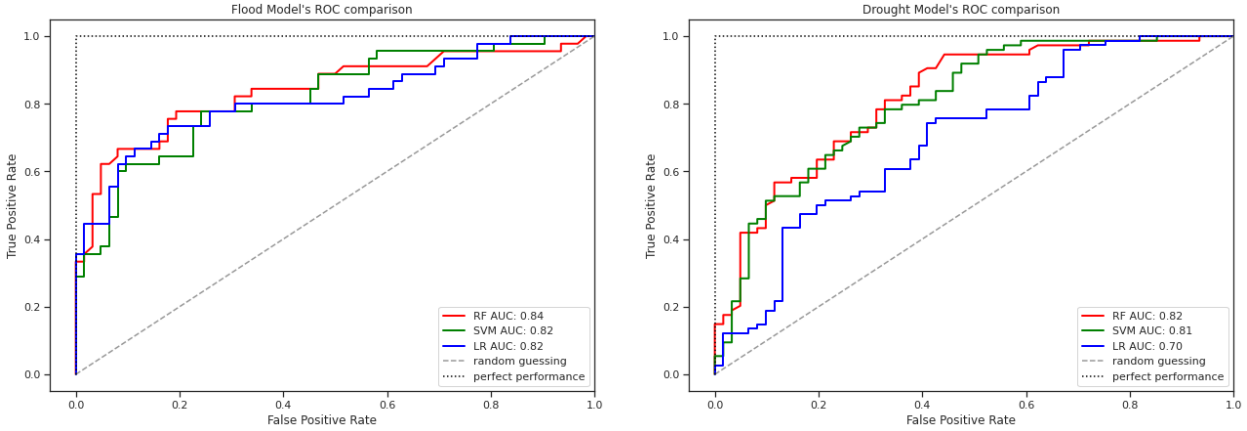

Figure 4: Validation of RF, SVM and LR models using ROC AUC for floods and droughts.

The susceptibility map presents the probability of correct (0 for low probability and 1 for high probability) prediction of flood and drought. The figure shows that the southern and northern regions are the most susceptible to flood and drought hazards. The most densely susceptible regions to flood are the Greater

Accra and the Upper East. The most densely susceptible regions to drought are the Central, the Western and the Upper West.

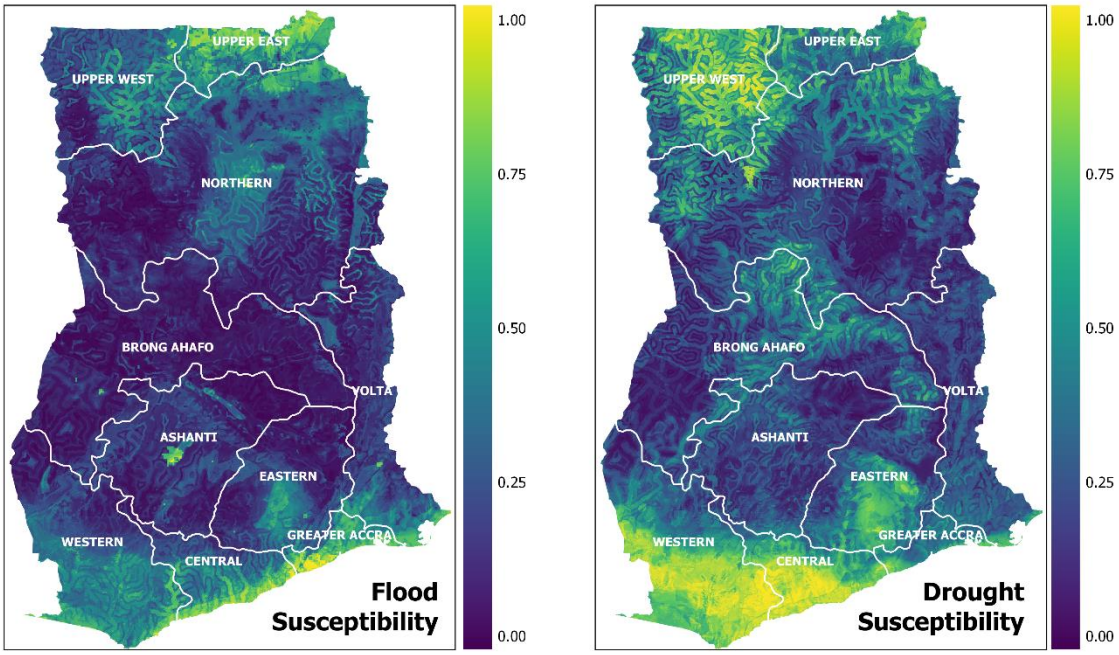

Figure 5 *Flood and drought susceptibility maps*

The most important features the RF model used in its predictions were temperature, topography and precipitation. The RF model used 30% of temperature, 23% of topography, 18% of land cover, 14% of precipitation, 11% of soil cover and 4% of hydrology data to predict the flood events. On the other hand, the RF model used 36% of temperature, 18% of topography, 17% of precipitation, 14% of soil cover, 10% of land cover and 5% of hydrology data to predict the drought events.

Vulnerability Analysis

The figure below presents Ghana's regions' sensitivity, adaptive capacity and vulnerability. The higher the sensitivity, the more sensible the population is to natural hazards. The most sensitive regions in Ghana are the Greater Accra, Northern, Upper West and Upper East. The higher the adaptive capacity, the better the population can recover from natural hazards. The Greater Accra, Central and Ashanti regions have the highest adaptive capacity. The higher the vulnerability, the more vulnerable the population is to natural hazards. Greater Accra is the most remarkable region of the bunch because despite being one of Ghana's most sensitive regions (due to the high percentage of marginal workers), its high adaptive capacity considerably reduces its vulnerability to natural hazards.

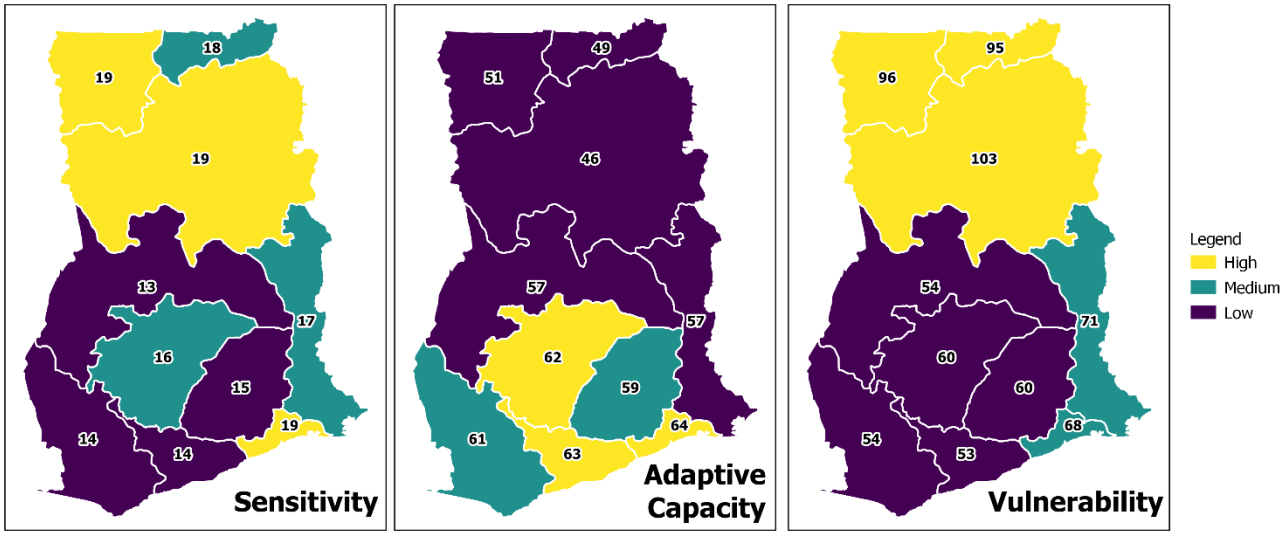

***Figure** 7: Ghana's regions sensitivity, adaptive capacity and vulnerability*

Hazard Risk Mapping

The analysis of the population density data emphasized population with a density greater than 40 persons per square km taking into account the remote populations in the risk analysis. Most of Ghana's surface has a population density greater than 40 persons per square km.

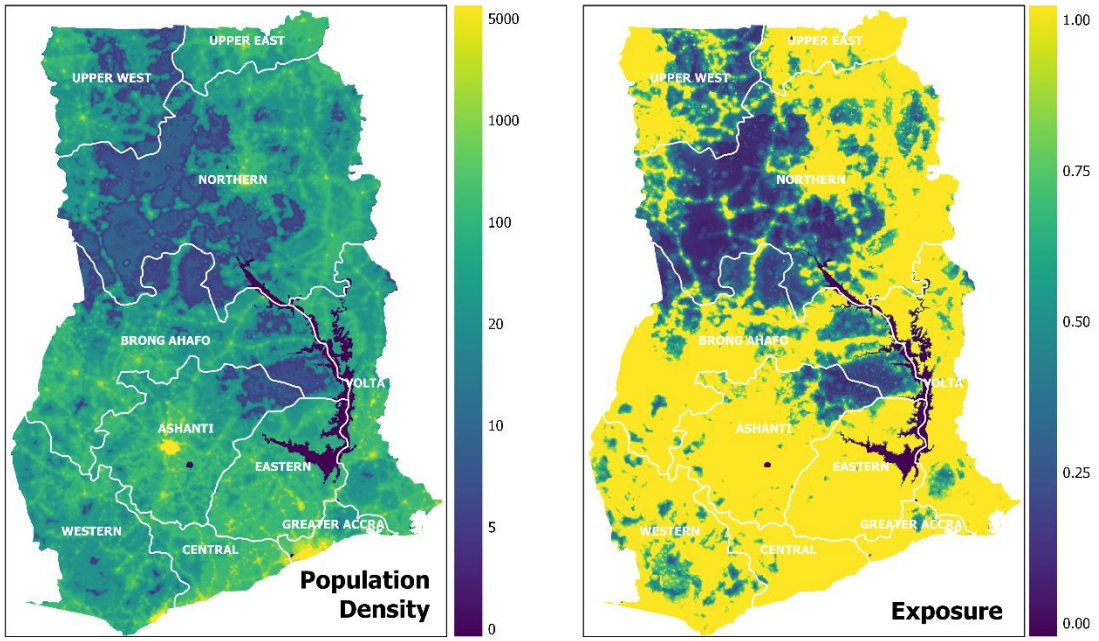

***Figure 8**:* Population density and exposure map.

It is without surprise that the hazard risk maps emphasize the hazards' susceptibilities depending on the most exposed and vulnerable population. The Upper East and Greater Accra are the most affected by the flood risks. The cities of Bolgatanga, Bawku, Kumasi and Tamale are also zones of critical flood risk. The Upper West, Upper East, Western and Central are the most affected regions for the drought risks.

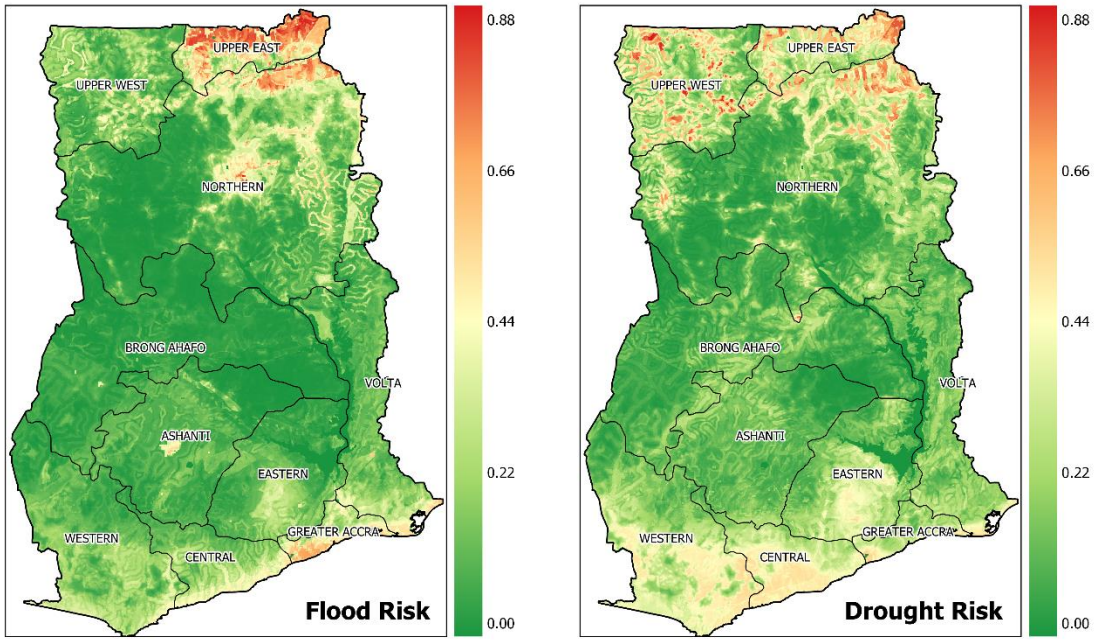

***Figure** 9: Flood and drought risk maps*

The hazards risk values were categorized into four groups: no hazard (areas with low risk, they range from 0 to 0.22 risk values), flood (areas with flood risk greater than 0.22), drought (areas with drought risk greater than 0.22) and both (intersection of flood and drought risk areas). The southern coasts and north of Ghana are the most impacted areas by floods and droughts. The upper east region of Ghana is the most affected region by both hazards. One-third and one-fourth of the country are impacted by drought and flood risks. There is a large area of overlapping flood and drought hazards because the ML model used for the susceptibility maps has nearly the same proportion of features.

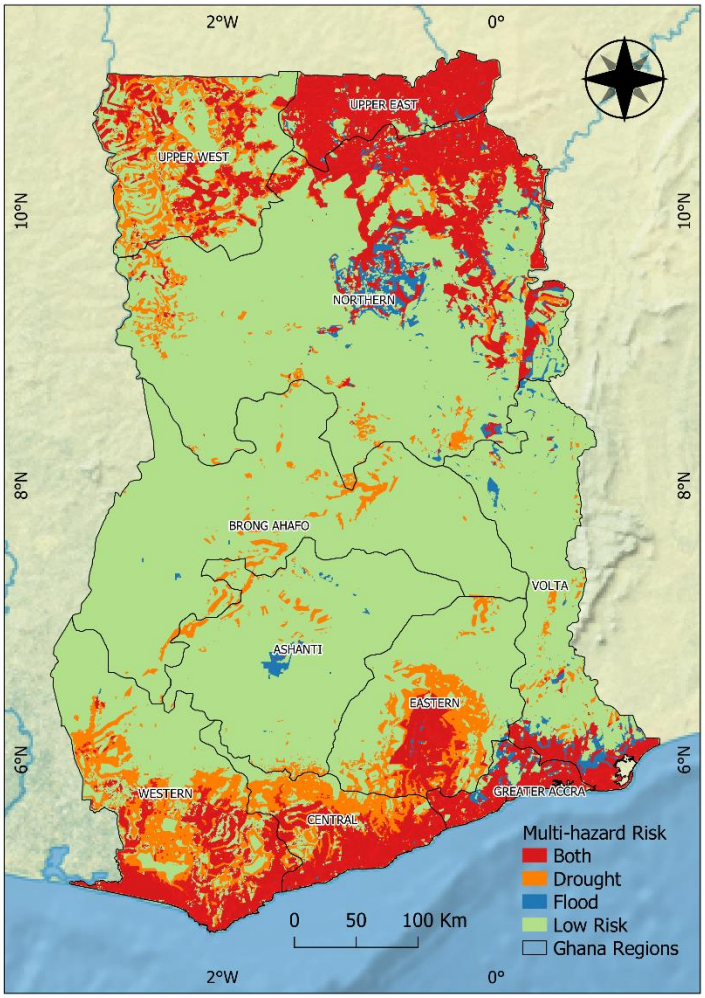

Figure 6: *Multi-hazard risk map*

Table 3: *Percentage of multi-hazard risks area*

	Moderate (%)	High (%)	Very High (%)	Total (%)
Both	11.21	3.66	1.42	16.29
Drought	14.81	2.12	0.15	17.08
Flood	3.58	0.65	0.06	4.29
Low Hazard Risk				62.34

Discussion

The main products of this study are flood and drought susceptibility, the population's vulnerability and exposure, and the multi-hazard risk maps. These maps show a distribution of floods and droughts susceptibility, population's vulnerability and exposure and multi-hazard risk. Antwi-Agyei used a similar

methodology to get the overall crop production vulnerability to drought in Ghana (Antwi-Agyei et al., 2011). In this work, the vulnerability of regions to drought is a function of the exposure to drought, the sensitivity of crop harvest to rainfall perturbations and the adaptive capacity of regions to cope with drought. The exposure index was defined as the degree to which a particular system is exposed to meteorological drought and corresponds to the drought susceptibility determined in this study. The zonal mean of the drought susceptibility values gives in the figure below.

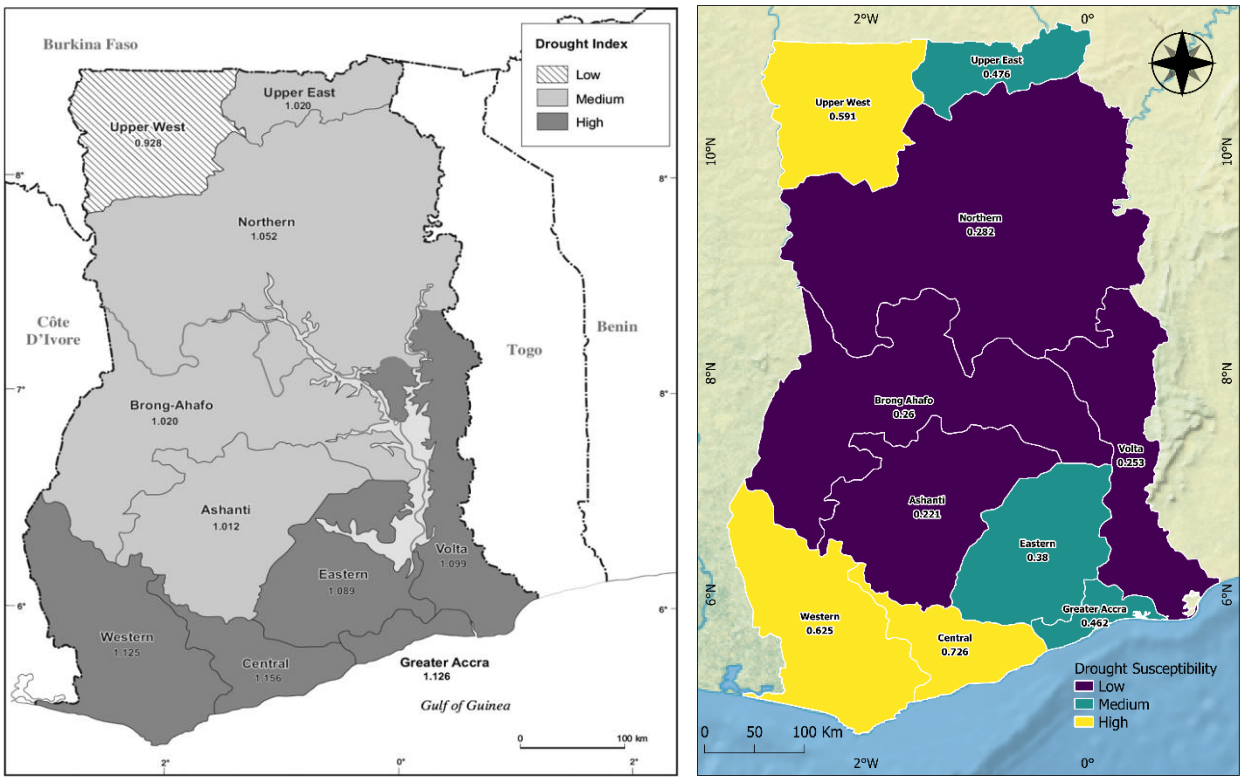

Figure 7: *Comparison between drought index and drought susceptibility*

The most obvious difference between these two drought maps is that the medium drought index regions became low drought susceptibility regions. Another difference is that the Upper West region changed from low to high drought susceptibility. The Western and Central regions remain areas of high drought susceptibility. Between 2000 and 2020, the drought susceptibility moved from the centre and Eastern areas of Ghana to its Western regions. This could be explained by the fact that Antwi-Agyei only relied on a ratio between the average of 30-year rainfall period for the 5 months (April-August) from 1971 to 2000 and each year's average rainfall for this period (April-August), while this study adopted a multivariate analysis of environmental factors including rainfall.

Another common factor in both studies is the population's adaptive capacity. Antwi-Agyei used the 2000 population and housing census data (Ghana Statistical Service, 2000) and considered only two variables: literacy rate and poverty rate. The map below shows that the population's adaptive capacity improves moving from the north to the South. Between 2000 and 2020, the adaptive capacity of the Southern population got obviously better.

Another obvious observation is that the less dense populations are located near the protected areas of Ghana. For example, the Western areas of the Northern region have the fewest population density due to the Mole National Park. Other less dense areas are also a result of other protected areas.

The ML models in this study performed as well as the other ML models found in the literature review. All the SVM and RF models developed by (Pourghasemi et al., 2020), (Rahmati et al., 2019), (Yousefi et al., 2020) and (Saha, 2021) had their AUC over 75%. In this study, only the baseline LR model had a performance of 70% AUC for drought classification but performed as good as the SVM model for flood classification. The RF and SVM had similar performances, with the RF performing slightly better for the flood and drought classification problems. Islam also found that this RF model performed 2 points better than his SVM model for flood classification (Islam, 2021). All this proves that the susceptibility maps resulting from this work are compliant with historical flood and drought events and could be relied on for disaster risk reduction policies and programs.

A limitation of this study was that it relied on SPI calculations to determine the drought events. Different results locations could be obtained using different indexes and monthly time steps. A more sophisticated drought index, the Standardized Precipitation Evapotranspiration Index (SPEI), is similar to SPI but integrates a temperature component. The performances of the ML models could also be improved by hyperparameter tuning or/and trying other ML models such as Dagging (Islam, 2021). A better subdivision of Ghana's administrative boundaries in the GSS survey could offer a more detailed vulnerability analysis. The use of districts instead of regions could improve the overall risk map. High resolutions of EO data could also improve the quality of the ML models, thus their susceptibility maps.

4. Conclusion

This study has mapped a multi-hazard risk map produced by determining flood and drought susceptibility and the population's vulnerability and exposure. ML models (LR, RF and SVM) were trained to classify flood and drought events with 6 earth observation features. The best-performing model was used to map the country's susceptibility to flooding and drought hazards. The population's vulnerability to natural

hazards was a product of the population's sensitivity and adaptive capacity based on socioeconomic surveys. The population's exposure to natural hazards was obtained by processing population density data.

The RF model was the best performing model, with a AUC of 0.84 for flood classification and 0.82 for drought classification and its most important features being the temperature, topography and precipitation. The susceptibility maps from this model revealed that the southern and northern regions are the most exposed to flood and drought hazards. The Northern regions have the most vulnerable population, and the areas the least exposed to natural hazards are the protected areas. This study establishes that the population of Northern and Southern Ghana live in areas of drought and flood risks, with one-third of the country impacted by drought and one-fourth impacted by the flood.

Flood and drought management strategies have recently been considered a top priority in Ghana. The present research provides valuable knowledge on flood and drought risk areas to help implement successful flood and drought mitigation strategies and land-use policy planning by local authorities and other parties. The interactive map resulting from this study makes the findings of this study easily accessible to policymakers.

Despite the milestone achieved in multi-hazard risk mapping in a West African country, further research must be done to improve this study. More investigation needs to be done to localize drought events in Ghana; other drought indexes and monthly time steps could be used. Other ML models could be associated with achieving higher-performing models, thus producing more accurate hazard susceptibility maps. Higher resolutions of EO datasets are also desired to improve the hazard susceptibility maps. Enhancing the spatial details of Ghana's socioeconomic surveys from region to district could also improve the vulnerability map. This work could also be extended and scaled for other African countries in need of a multi-hazard risk map.

Reference

Abu Reza Md Towfiqul Islam, Swapan Talukdar, Susanta Mahato, Sonali Kundu, Kutub Uddin Eibek, Quoc Bao Pham, Alban Kuriqi, Nguyen Thi Thuy Linh, Flood susceptibility modelling using advanced ensemble machine learning models, Geoscience Frontiers, Volume 12, Issue 3, 2021, 101075, ISSN 1674-9871, https://doi.org/10.1016/j.gsf.2020.09.006.

Al-Hassan, Ramatu & Kuwornu, John. (2013). Application of Livelihood Vulnerability Index in Assessing Vulnerability to Climate Change and Variability in Northern Ghana.

Amekudzi, L.K.; Yamba, EI; Preko, K.; Asare, E.O.; Aryee, J.; Baidu, M.; Codjoe, S.N. Variabilities in rainfall onset, cessation and length of rainy season for the various Agro-Ecological Zones of Ghana. Climate 2015, 3, 416–434.

Batjes, Niels. (2010). IPCC default soil classes derived from the Harmonized World Soil Data Base (ver. 1.1).

Bera, A., Gowhar, M., Shruti, K., Majid, F., Suraj, K. S., Netrananda, S., & Pankaj, K. (2022). Vulnerability and Risk Assessment to Climate Change in Sagar Island, India. Water 14, no. 5: 823. https://doi.org/10.3390/w14050823.

Bisong, E. (2019). Google Colaboratory. In: Building Machine Learning and Deep Learning Models on Google Cloud Platform. Apress, Berkeley, CA. https://doi.org/10.1007/978-1-4842-4470-8_7.

Braun, von, J. 2008. Responding to the world food crisis: Getting on the Right Track. IFPRI Report. Washington, DC: International Food Policy Research Institute.

Dee, D.P., Uppala, S.M., Simmons, A.J., Berrisford, P., Poli, P., Kobayashi, S., Andrae, U., Balmaseda, M.A., Balsamo, G., Bauer, P., Bechtold, P., Beljaars, A.C.M., van de Berg, L., Bidlot, J., Bormann, N., Delsol, C., Dragani, R., Fuentes, M., Geer, A.J., Haimberger, L., Healy, S.B., Hersbach, H., Hólm, E.V., Isaksen, L., Kållberg, P., Köhler, M., Matricardi, M., McNally, A.P., Monge-Sanz, B.M., Morcrette, J.-J., Park, B.-K., Peubey, C., de Rosnay, P., Tavolato, C., Thépaut, J.-N. and Vitart, F. (2011), The ERA-Interim reanalysis: configuration and performance of the data assimilation system. Q.J.R. Meteorol. Soc., 137: 553-597. https://doi.org/10.1002/qj.828.

EM-DAT (2008). EM-DAT: The International Disaster Database Available www.emdat.be/Database/Trends/trends.html.

FloodList (2022). Website of global flood reports. https://floodlist.com.

Funk, C. et al. The climate hazards infrared precipitation with stations—a new environmental record for monitoring extremes. Sci. Data. 2:150066 doi: 10.1038/sdata.2015.66 (2015).

Füssel, HM., Klein, R.J.T. Climate Change Vulnerability Assessments: An Evolution of Conceptual Thinking. Climatic Change 75, 301–329 (2006). https://doi.org/10.1007/s10584-006-0329-3.

Ghana Statistical Service. (2000). Population and housing census (2000). Accra, Ghana: Ghana Government.

Ghana Statistical Service (2019). Main report. https://www.statsghana.gov.gh/gssmain/fileUpload/pressrelease/GLSS7%20MAIN%20REPORT_FINAL.pdf.

Ghana Statistical Service (2022). Ghana 2021 Population and Housing Census. General Report Volume 3A: Population of Regions and Districts.

https://statsghana.gov.gh/gssmain/fileUpload/pressrelease/2021%20PHC%20General%20Report%20Vol%203A_Population%20of%20Regions%20and%20Districts_181121.pdf

Global Administrative Areas (2012). GADM database of Global Administrative Areas, version 2.0. [online] URL: www.gadm.org.

Global Land Cover 2000 database. European Commission, Joint Research Centre, 2003.

Hajian-Tilaki K. Receiver Operating Characteristic (ROC) Curve Analysis for Medical Diagnostic Test Evaluation. Caspian J Intern Med. 2013 Spring;4(2):627-35. PMID: 24009950; PMCID: PMC3755824.

Hamid Reza Pourghasemi, Amiya Gayen, Mohsen Edalat, Mehrdad Zarafshar, John P. Tiefenbacher. Is multi-hazard mapping effective in assessing natural hazards and integrated watershed management?, Geoscience Frontiers Volume 11, Issue 4, 2020, Pages 1203-1217, ISSN 1674-9871, https://doi.org/10.1016/j.gsf.2019.10.008.

Harris, C.R., Millman, K.J., van der Walt, S.J. et al. Array programming with NumPy. Nature 585, 357–362 (2020). DOI: 10.1038/s41586-020-2649-2. (Publisher link).

Hoyer, S., & Joseph, H. (2017). xarray: N-D labeled Arrays and Datasets in Python. Journal of Open Research Software, 5(1). https://doi.org/10.5334/jors.148.

IPCC, 2022: Summary for Policymakers [H.-O. Pörtner, D.C. Roberts, E.S. Poloczanska, K. Mintenbeck, M. Tignor, A. Alegría, M. Craig, S. Langsdorf, S. Löschke, V. Möller, A. Okem (eds.)]. In: Climate Change 2022: Impacts, Adaptation, and Vulnerability. Contribution of Working Group II to the Sixth Assessment Report of the Intergovernmental Panel on Climate Change [H.-O. Pörtner, D.C. Roberts, M. Tignor, E.S. Poloczanska, K. Mintenbeck, A. Alegría, M. Craig, S. Langsdorf, S. Löschke, V. Möller, A. Okem, B. Rama (eds.)]. Cambridge University Press. In Press.

Jarvis A., H.I. Reuter, A. Nelson, E. Guevara, 2008, Hole-filled seamless SRTM data V4, International Centre for Tropical Agriculture (CIAT), available from https://srtm.csi.cgiar.org.

Kabo-Bah, A.T.; Diji, C.J.; Nokoe, K.; Mulugetta, Y.; Obeng-Ofori, D.; Akpoti, K. Multiyear Rainfall and Temperature Trends in the Volta River Basin and their Potential Impact on Hydropower Generation in Ghana. Climate 2016, 4, 49. https://doi.org/10.3390/cli4040049.

Kelsey Jordahl, Joris Van den Bossche, Martin Fleischmann, Jacob Wasserman, James McBride, Jeffrey Gerard, … François Leblanc. (2020, July 15). geopandas/geopandas: v0.8.1 (Version v0.8.1). Zenodo. http://doi.org/10.5281/zenodo.3946761.

Langaas, S. (1995). Completeness of the Digital Chart of the World (DCW) database. UNEP/GRID-Arendal.

Omid Rahmati, Fatemeh Falah, Kavina Shaanu Dayal, Ravinesh C. Deo, Farnoush Mohammadi, Trent Biggs, Davoud Davoudi Moghaddam, Seyed Amir Naghibi, Dieu Tien Bui, Machine learning approaches for spatial modeling of agricultural droughts in the south-east region of Queensland Australia, Science of The Total Environment, Volume 699, 2020, 134230, ISSN 0048-9697, https://doi.org/10.1016/j.scitotenv.2019.134230.

Pawley (2020). Pyspatialml: Machine learning for GIS spatial modelling. https://pypi.org/project/pyspatialml/.

Philip Antwi-Agyei, Evan D.G. Fraser, Andrew J. Dougill, Lindsay C. Stringer, Elisabeth Simelton. Mapping the vulnerability of crop production to drought in Ghana using rainfall, yield and socioeconomic data, Applied Geography, Volume 32, Issue 2, 2012, Pages 324-334, ISSN 0143-6228, https://doi.org/10.1016/j.apgeog.2011.06.010.

Rahmati, Omid, Saleh Yousefi, Zahra Kalantari, Evelyn Uuemaa, Teimur Teimurian, Saskia Keesstra, Tien D. Pham, and Dieu Tien Bui. 2019. "Multi-Hazard Exposure Mapping Using Machine Learning Techniques: A Case Study from Iran" Remote Sensing 11, no. 16: 1943. https://doi.org/10.3390/rs11161943.

Rehman, S., Sahana, M., Hong, H. et al. A systematic review on approaches and methods used for flood vulnerability assessment: framework for future research. Nat Hazards 96, 975–998 (2019). https://doi.org/10.1007/s11069-018-03567-z.

Scikit-learn: Machine Learning in Python, Pedregosa et al., JMLR 12, pp. 2825-2830, 2011.

Sunil Saha and Amiya Gayen and Priyanka Gogoi and Barnali Kundu and Gopal Chandra Paul and Biswajeet Pradhan, Proposing novel ensemble approach of particle swarm optimized and machine learning algorithms for drought vulnerability mapping in Jharkhand, India, Geocarto International, 0, 0, 1-32, 2021, 10.1080/10106049.2021.1989500.

Tappan, G. G., Cushing, W.M., Cotillon, S.E., Mathis, M.L., Hutchinson, J.A., Herrmann, S.M., and Dalsted, K.J., 2016, West Africa Land Use Land Cover Time Series: US Geological Survey data release, http://dx.doi.org/10.5066/F73N21JF.

UN (United Nations). 2011. International Strategy for Hazard Reduction. Effective Measures to Build Resilience in Africa to Adapt to Climate Change. Briefing note 04. Geneva, Switzerland: UNISDR.

van Niekerk, D., & Nemakonde, L. Natural Hazards and Their Governance in Sub-Saharan Africa. Oxford Research Encyclopedia of Natural Hazard Science. Retrieved 14 Jul. 2022, from https://oxfordre.com/naturalhazardscience/view/10.1093/acrefore/9780199389407.001.0001/acrefore-9780199389407-e-230.

WorldPop (www.worldpop.org - School of Geography and Environmental Science, University of Southampton; Department of Geography and Geosciences, University of Louisville; Departement de Geographie, Universite de Namur) and Center for International Earth Science Information Network (CIESIN), Columbia University (2018). Global High Resolution Population Denominators Project - Funded by The Bill and Melinda Gates Foundation (OPP1134076). https://dx.doi.org/10.5258/SOTON/WP00675.

World Bank Group (2016). Striving Toward Disaster Resilient Development in Sub-Saharan Africa Strategic Framework 2016–2020.

Yousefi, S., Pourghasemi, H.R., Emami, S.N. et al. A machine learning framework for multi-hazards modeling and mapping in a mountainous area. Sci Rep 10, 12144 (2020). https://doi.org/10.1038/s41598-020-69233-2.